A Dynamical Model of Kinesin-Microtubule Motility Assays

Frank Gibbons,* Jean-François Chauwin,* Marcelo Despósito,*† and Jorge V. José*
*Physics Department, and Center for Interdisciplinary Research on Complex Systems, Northeastern University, Boston, Massachusetts 02115, USA and †Departamento de Física, Facultad de Ciencias Exactas y Naturales, Universidad de Buenos Aires, RA-1428 Buenos Aires, Argentina

ABSTRACT A two-dimensional stochastic model for the dynamics of microtubules in gliding-assay experiments is presented here, which includes the viscous drag acting on the moving fiber and the interaction with the kinesins. For this purpose, we model kinesin as a spring, and explicitly use parameter values to characterize the model from experimental data. We numerically compute the mean attachment lifetimes of all motors, the total force exerted on the microtubules at all times, the effects of a distribution in the motor speeds, and also the mean velocity of a microtubule in a gliding assay. We find quantitative agreement with the results of J. Howard, A. J. Hudspeth, and R. D. Vale, *Nature*. 342:154–158. We perform additional numerical analysis of the individual motors, and show how cancellation of the forces exerted by the many motors creates a resultant longitudinal force much smaller than the maximum force that could be exerted by a single motor. We also examine the effects of inhomogeneities in the motor-speeds. Finally, we present a simple theoretical model for microtubules dynamics in gliding assays. We show that the model can be analytically solved in the limit of few motors attached to the microtubule and in the opposite limit of high motor density. We find that the speed of the microtubule goes like the mean speed of the motors in good quantitative agreement with the experimental and numerical results.

INTRODUCTION

Molecular motors constitute a class of proteins responsible for the many transport processes within eukaryotic cells, and in the organization of the mitotic spindle (see Alberts et al., 1994 or Lodish et al., 1995 for a general introduction). Motors can be characterized as consisting of three domains: the "head" or "motor" domain, in which force is produced, the "tail" which attaches to a load, and the "body," which links the head to the tail. These motors work by moving their motor domains along relatively rigid polymers with a load attached to their tails. They are commonly divided into three families, myosins, dyneins, and kinesins (see Hirokawa, 1998 for a family tree). Myosins are associated with actin filaments, whereas kinesins and dyneins are associated with microtubules (MTs). These motor proteins have been the subject of many ingenious experiments, as attempts to characterize them have grown more ambitious. The discovery of the kinesin family in the late 1980s (Hirokawa et al., 1989; Scholey et al., 1989), along with advances in imaging technology, opened the door to a set of exciting experiments. In gliding motility assays (Howard et al., 1989; Hancock and Howard, 1998), a microscope slide is coated with kinesin, a microtubule placed on top of the slide, and the motion of the center of mass of the MT is tracked as a function of time. In the optical-tweezer assay (Block et al., 1990), a single motor is tethered to a latex bead, which is then held in an optical potential well. Attempts by the motor to drag the bead out of the well yield important quantitative information about the motor's force. These motor assays allowed the recording of the position (Howard et al., 1989; Block et al., 1990; Svoboda et al., 1993), velocity (Block et al., 1990), and force (Finer et al., 1994) applied by a single motor, all with unprecedented sensitivity.

As a more complete characterization of kinesin motors emerged, a number of questions became apparent. First, how do these motors move? Some kind of walking model is believed to be the correct way to think about this (Peskin and Oster, 1995; Derényi and Vicsek, 1996; Vicsek, 1997). Second, the "fuel" used by these motors is well known, but the question of the stochiometry between fuel consumption and steps walked has recently been answered by Hua et al., (1997), Schnitzer and Block (1997), and Coy et al. (1999), who have shown that consumption of one ATP molecule results in kinesin taking exactly one 8-nm step. Third, in gliding assays, the speed of microtubule movement is found to be independent of both the length of the microtubule, and the density of kinesin adsorbed onto the substrate (Howard et al., 1989; Hancock and Howard, 1998). It is not fully understood why this should be so. And last, a graph of speed versus kinesin density tells us very little about the behavior of a single motor—how long does it remain attached to the microtubule, how much force does it exert, how is it correlated with the behavior of the others, etc.

In this work, we focus on the last two of these questions. For this purpose, we develop a stochastic model for the dynamics of a microtubule in gliding assay experiments, which includes the viscous drag acting on the moving fiber and the interaction with the kinesins. For those motors, we construct a simple mechanical model extracting the involved constants based on experimental data. We show how our model quantitatively reproduces the results of the gliding-assay experiments of Howard et al. (1989) and Hancock and Howard (1998). Having established the validity of the

Received for publication 21 July 2000 and in final form 5 March 2001.

Address reprint requests to Jorge Jose, Center for the Interdisciplinary Research on Complex Systems, Northeastern University, 360 Huntington Avenue, Boston, MA 02115. Tel.: 617-373-2927; Fax: 617-373-2943; E-mail: jjv@neu.edu.

0006-3495/01/06/2515/12 $2.00

model, we then examine various aspects of motor behavior to try to understand these observations. We use a combination of detailed numerical calculations with analytic analysis in different limits.

THE MODEL

We describe the dynamics of a MT in terms of the location of its center of mass $\vec{R} = x\hat{\imath} + y\hat{\jmath}$ (where $\hat{\imath}$ and $\hat{\jmath}$ are units vectors along the x and y axes), and the angle Θ between the horizontal x-axis and the unit vector pointing along the MT.

This model is two-dimensional, because it has been shown (Hunt and Howard, 1993) that, in motility assays at least, the vertical distance between the head and tail of a kinesin attached to a microtubule is only about 20% of its total length—in other words, the motors mostly lie in a plane parallel to the microscope slide. The motion of the microtubule is overdamped because it involves low Reynolds numbers (Hunt and Howard, 1993). This dimensionless number, defined as $\mathcal{R} \equiv vL\rho/\eta$, where v is the relative velocity between the object and the fluid, L is its dimension, ρ and η are, respectively, the density and viscosity of the fluid, indicating the relative importance of inertial to viscous effects. For a fish swimming in water, $\mathcal{R} \simeq 100$, whereas, for a microtubule moving in an aqueous solution, $\mathcal{R} \simeq 8 \times 10^{-6}$, clearly indicating that, although the fish experiences inertia, the MT does not. Its motion is Aristotelian rather than Newtonian. A nice introduction to this concept is given in Purcell (1977) and Berg (1983).

Therefore, neglecting inertial effects, the translational bidimensional Brownian motion is described by the Langevin equation

$$\vec{f} = \vec{F} + \vec{\eta}_t(t), \tag{1}$$

whereas, for the rotational Brownian motion, we have

$$\zeta_r\dot{\Theta} = \tau + \eta_r(t), \tag{2}$$

where the dot means the time derivative, $\vec{f}$ is the translational drag force, ζ_r is the rotational friction constant, $\vec{F}$ is the applied external force by the molecular motors on the MT, and τ is the associated torque. The translational and rotational Gaussian fluctuating Langevin forces are respectively denoted by $\vec{\eta}_t(t)$ and $\eta_r(t)$.

In what follows, we assume that the motors are located randomly in the plane, with the position of the ith motors tail fixed at $\vec{r}_i$ and the position of the head at $\vec{h}_i$. (See Fig. 1 for schematic.) We model each motor as a simple spring, parameterized by a spring constant k_s and equilibrium length L_0. Each motor will exert a force on the MT equal to (see Appendix for further justification for our model)

$$\vec{F}_i = -k_s(\vec{h}_i - \vec{r}_i). \tag{3}$$

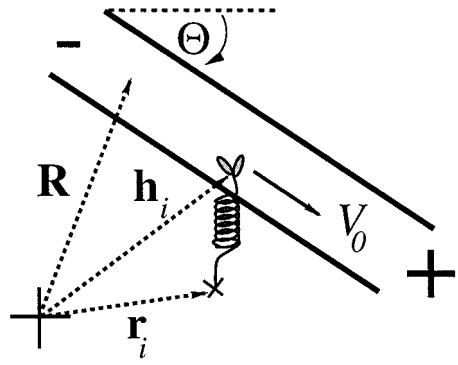

FIGURE 1 A schematic of a motor walking on a microtubule, indicating the position of the center of mass of the microtubule $\vec{R}$, the (fixed) tail of the ith motor at $\vec{r}_i$ and the moving head at $\vec{h}_i$. Kinesin is a plus-end-directed motor, as indicated by the arrow marked v_0. Note that only a small section of the microtubule is shown, because it is so much larger than the motor.

The components of the force exerted by the spring parallel and perpendicular to the MT axis along the unitary vector $\hat{\vec{u}}$ are

$$F_\parallel = \vec{F}\cdot\hat{\vec{u}} = -k_s\hat{\vec{u}}\cdot(\vec{h}_i - \vec{r}_i),$$
$$F_\perp = \vec{F} - (\vec{F}\cdot\hat{\vec{u}})\hat{\vec{u}}, \tag{4}$$

whereas the magnitude of the torque is given by

$$\tau_i = |\vec{h}_i - \vec{R}|F_i\sin\phi_i, \tag{5}$$

where ϕ_i is the angle between the rod and the spring.

Combining Eqs. 1–5, we have (see Appendix for more details)

$$\dot{x} = \frac{D_\parallel}{k_BT}[F_\parallel\cos\Theta - 2F_\perp\sin\Theta] + \vec{\eta}_t(t)\cdot\hat{\imath},$$
$$\dot{y} = \frac{D_\parallel}{k_BT}[F_\parallel\sin\Theta + 2F_\perp\cos\Theta] + \vec{\eta}_t(t)\cdot\hat{\jmath},$$
$$\dot{\Theta} = \frac{D_r}{k_BT}k_s\left(\sum_i{}'|\vec{h}_i - \vec{R}||\vec{h}_i - \vec{r}_i|\sin\phi_i\right) + \eta_r(t), \tag{6}$$

where Σ_i' denotes a sum only over those motors that are attached to the MT, and $\hat{\imath}$, $\hat{\jmath}$ are unitary vectors along the x and y axes, respectively.

In Table 1, we show the parameter values that we use to model the behavior of the motors, as determined from

Table 1 Parameter values used in the simulations

Microtubule length L	10 μm
Microtubule diameter b	25 nm
Spring constant for motor, k_s	0.2 pN nm^{-1}
Equilibrium length for spring, L_0	50 nm
Maximal (unloaded) motor speed, v_0	800 nm s^{-1}
Motor stall force, F_{stall}	5 pN
Capture parameter, w	40 nm

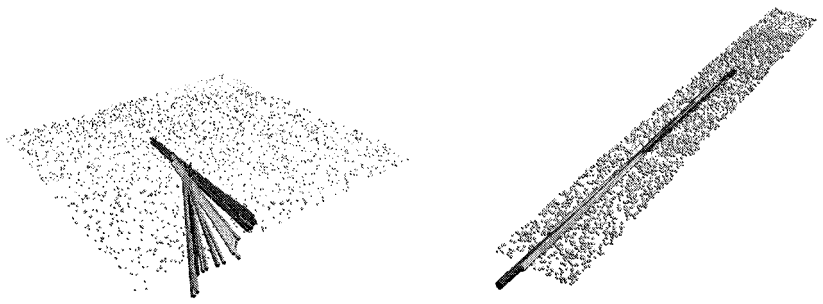

(a) Low kinesin density ($\sigma_{kin} = 5\mu m^{-2}$)

(b) High kinesin density ($\sigma_{kin} = 100\mu m^{-2}$)

FIGURE 2 Illustration of results from simulation of microtubule gliding assays at (*A*) low kinesin density ($\sigma_{kin} = 5\ \mu m^{-2}$) and (*B*) high kinesin density ($\sigma_{kin} = 100\ \mu m^{-2}$). At sufficiently high densities, the Brownian angular fluctuations are damped, and the motion is in a straight line. The MT is represented by the long rod (its color changes from dark to light, to represent the passage of time). The locations of the motors are indicated by the small spheres.

experiment. A typical length L for an MT in the mitotic spindle is 10 microns (Gliksman et al., 1993). In the gliding-assay experiments of Howard et al., the length of the MT is $2.2 \pm 1.4\ \mu m$ (Howard et al., 1989) using bovine brain kinesin and $2.05 \pm 0.92\ \mu m$ (Hancock and Howard, 1998) using recombinant *Drosophila* kinesins. The spring constant k_s is taken from experimental work (Coppin et al., 1995). The value of the equilibrium length L_0 of the spring is based on the facts that the length of kinesin is about 80 nm, and the extension of the spring, which is sufficient to stall the motor, is about 25 nm. A precise value for the unloaded motor velocity v_0 is not known (see Howard et al., 1989; Svoboda et al., 1993), but it is in the range 0.5–1.0 $\mu m\ s^{-1}$. The parameter w describes the minimal proximity required between a motor and the microtubule for capture to occur. No experimental values exist, but clearly it should be no larger than the equilibrium length of the motor itself ($\sim$80 nm).

NUMERICAL RESULTS

In Fig. 2, we show a gliding assay picture, obtained from our numerical results for the MT motion at different times for low and high kinesin densities. There we see that, at low densities, the MT can rotate as it moves, whereas, at high densities, the rotation is quenched.

We also looked at the shape of the trajectories of the center of mass of the MT, as a function of kinesin density, σ_{kin}. Figure 3 shows typical trajectories as a function of kinesin density, using the parameters in Table 1. For some densities between $\sigma_{kin} = 1\ \mu m^{-2}$ and $\sigma_{kin} = 5\ \mu m^{-2}$, there is clearly a crossover from Brownian motion to a more directed kind of motion, in which the angular fluctuations are damped out. This critical density has been predicted (Duke et al., 1995) to be $\sigma^{**}_{kin} \sim 0.05\ \mu m^{-2}$, independent of microtubule length. However, their calculation assumes a finite persistence length for the microtubules of $\sim$5 nm, whereas our simulations assume the rods are completely rigid (infinite persistence length). Therefore, the critical density in our analysis should be larger.

We have performed about 300 realizations of the gliding-assay simulations, each with a different initial random arrangement of kinesins, and random initial position and orientation of the MT. For all realizations at a given density, we drew graphics like Figs. 3 and 4, ensuring that the track was straight, and then computing the average speed of the MT, as $\langle v(\sigma_{kin})\rangle \equiv (d(t) - d(0))/t$, where $d(t)$ is the distance of the center of mass displacement at time t from its initial position $d(0)$. We also computed error bounds for each $\langle v(\sigma_{kin})\rangle$. The results are shown in Fig. 5. Our principal finding, in agreement with experiment, is that the speed of the microtubule remains constant over approximately two orders of magnitude in the kinesin density, σ_{kin} (i.e., from $\sigma_{kin} = 2\ \mu m^{-2}$ to $\sigma_{kin} = 200\ \mu m^{-2}$). For densities less than $\sigma_{kin} = 1\ \mu m^{-2}$, we find it difficult to gather data, because the motors are so few and far between that there is seldom any directed motion. At densities beyond $\sigma_{kin} = 200\ \mu m^{-2}$, the opposite is true—there are so many motors that the

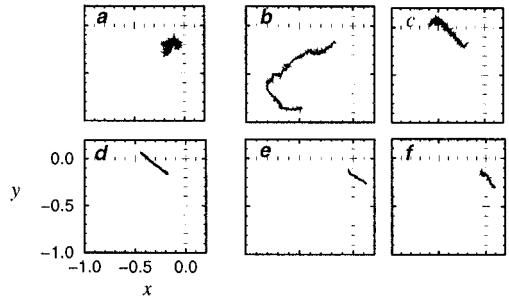

FIGURE 3 Comparison of typical trajectories for $w = 40$ nm, as the kinesin density is varied. Initial conditions are unchanged in each run. *Panels a–f* correspond to densities of $\sigma_{kin} = 0.1, 1.0, 5.0, 20.0, 60.0, 100.0\ \mu m^{-2}$, respectively. Note that not all trajectories represent equal lapses in time.

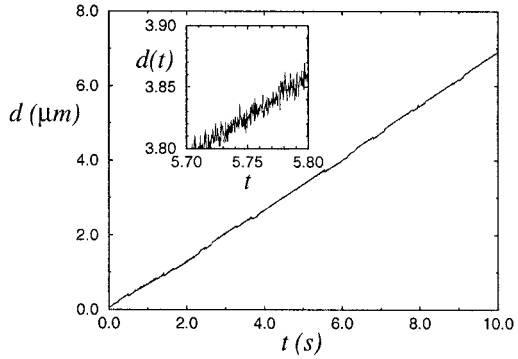

FIGURE 4 Typical data for $d(t)$, the distance moved by the MT center of mass, from its initial position, as a function of time t. The inset shows the path taken by the MT center of mass, as it moves across the (*square*) slide. The microtubule length is 10 μm, so, clearly, the microtubule has moved by almost its own length in this simulation. The speed of the microtubule is clearly constant for the length of the simulation. Here $\sigma_{kin} = 10\ \mu m^{-2}$. Inset shows the expected noisy nature of the same data.

simulation time-step is driven down by orders of magnitude, causing the simulations to be impracticably slow.

A possible partial explanation for this: first, we consider low kinesin densities ($\sigma_{kin} \lesssim 5\ \mu m^{-2}$). With only one motor attached (on average) at a given time, it is impossible for the microtubule to move faster than the motor can walk. For medium kinesin densities ($5 < \sigma_{kin} < 50\ \mu m^{-2}$), there may be only two or three motors attached, so there is a finite probability that they will cooperate with each other. At high kinesin densities ($50 < \sigma_{kin} \lesssim 200\ \mu m^{-2}$), there is a larger

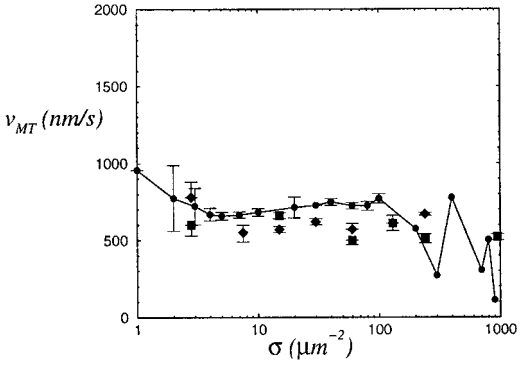

FIGURE 5 Comparison of the results obtained by simulation using the parameters of Table 1, with those experimentally obtained by Howard's group. Simulated data represent 257 individual MTs. In the experiments by Howard et al. (1989), the results came from measurements of drawings by hand on acetate-sheet overlays of taped video images, acquired at 33 ms intervals. At low kinesin density, the speed was determined as the rate at which the MT's trailing end approached the fixed point at which the kinesin molecule was located. Results were averaged over 233 individual MTs in two different experiments (hence different symbols), and error bars correspond to standard errors of the means. The experimental data is taken from Howard et al. (1989) that used bovine brain kinesin. These results are very similar to those obtained using two-headed recombinant *Drosophila* kinesins (Hancock and Howard, 1998). See text for a more detailed discussion of this figure.

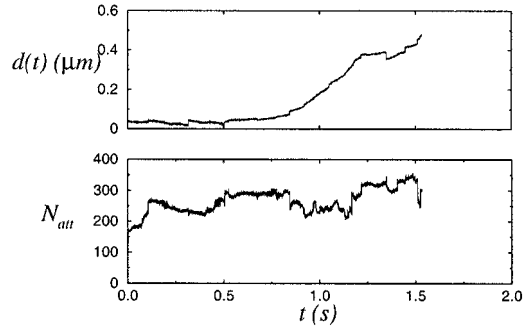

FIGURE 6 Typical microtubule path at high kinesin density, from simulation, showing the attachment phase, followed by waiting, and finally directed motion. The weakness of the data shown in this graph is in the length of time simulated. The MT moves only a few tenths of a micron, whereas its own length is 10 microns. Movement on this scale would not be easily detectable in an experiment.

number of motors attached, and it is likely to have some averaging out, with some motors pushing and others pulling. It is interesting to examine the detailed dynamics of the initial attachment of motors to the microtubule. An example is shown in Fig. 6. At low densities, there is a brief "attachment" phase, as the motors attach themselves to the microtubule. The number of motors attached rapidly reaches a relatively constant value, and the microtubule begins to move. At higher kinesin densities, the attachment phase happens rapidly too, but motion does not begin immediately. There may be a waiting period, during which the microtubule undergoes no directed motion. It simply sits, buffeted by the Brownian noise. This is visible in Fig. 6, for $t < 0.7$ s. This kind of behavior can be explained by our theoretical model (see below).

Analysis of the effective force

There are two questions here that are worth looking at: what is the force required to move an MT? and why is the speed such a weak function of kinesin density? Or, to use a well known analogy (Leibler and Huse, 1993), why should a boat with 8 rowers move no faster than one with 4?

A simple back-of-the-envelope calculation provides a qualitative answer to the first question. Let us take Eq. 6 and assume an MT aligned and moving only along the x-axis. Take the time average of both sides of Eq. 6 (which eliminates the noise term, by definition), and ask what is the time-averaged longitudinal force necessary to produce the observed velocity. The force is given by $\langle F \rangle = k_B T \langle \dot{x} \rangle / D_{\|}$. Taking $k_B T = 4.1 \times 10^{-21}$ J, $\langle \dot{x} \rangle = 650$ nm s^{-1} (see Fig. 5) and $D_{\|} = 10^{-13}$ m^2 s^{-1}, we find $\langle F \rangle \sim 0.027$ pN. Analysis of the force exerted during our simulations shows a figure within a factor of two of this force (see Fig. 7). However, as we can see from a simple force–velocity curve (Fig. 8), the maximum force that a single motor can exert is larger than this by a factor of 100 and up to 5 pN. A more detailed

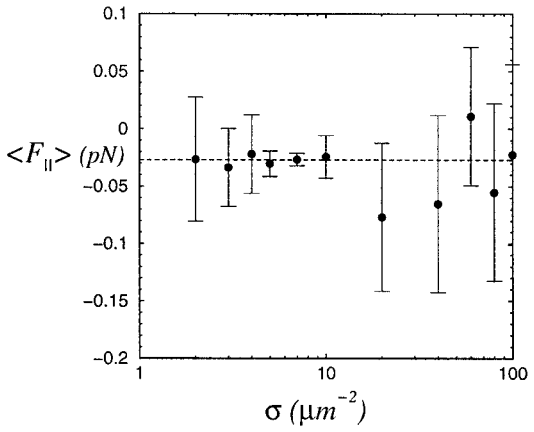

FIGURE 7 The time-averaged total force exerted by motors on a microtubule. Black circles indicate ensemble means, error bars indicate standard deviations of the ensemble ($\sigma^2_{\text{ens}} = (1/N)\ \Sigma_{i=1,N}\ \sigma_i^2$). Negative values indicate that the force is directed toward the minus end of the microtubule, which is consistent with motors walking toward the plus end. The force necessary to propel a microtubule at the observed averaged speed of ~650 nm s^{-1} is −0.027 pN.

analysis given in the Appendix leads to an answer that agrees quantitatively with the numerical calculations.

We note that the mean force exerted at all densities is extremely small, much smaller than the maximum force exerted by a single motor. This distribution of forces is important to understand the kinesin density independence of the average MT velocity. Of course, the distribution of forces exerted at a given time varies as a function of density σ_{kin}. This variation is explicitly shown in Fig. 9, which gives a Gaussian distribution of forces exerted on the MT over the length of a numerical run. The force changes as a function of the longitudinal force exerted in the MT. Here we show results for several densities: $\sigma_{\text{kin}} = 5$, 10, 20, 30, 50, and 100 μm^{-2}. We point out that the results for densities below 130 μm^{-2} have error bars due to the ensemble of different initial conditions, but for higher densities the calculations are very CPU intensive, and we only show the results for one initial condition. These results, however, follow qualitatively and even quantitatively the experimental results.

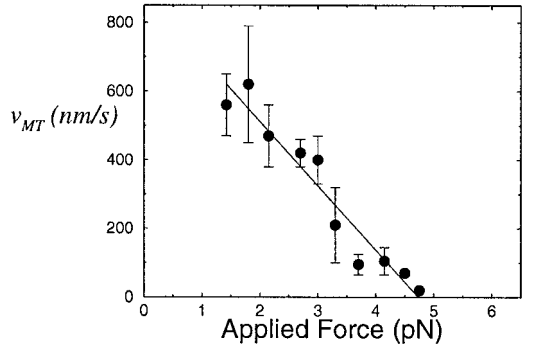

FIGURE 8 A typical experimentally determined force–velocity curve for kinesin, taken from Svoboda et al. (1993). For low values of the applied force (the load), the velocity is near its maximum value. The velocity decreases as the load increases, until the stall force F_{stall} is reached and the velocity is zero. Under loads greater than the stall force, the tendency is for the motor to become detached from the microtubule, rather than to move backward.

Attachment lifetime analysis

We have also examined the distribution in times for which each motor remains attached to the microtubule, shown in Fig. 10. The times shown may include several detachment and reattachment processes. What matters is the total length of time a motor is attached, whether continuously or not. We find that, of all the motors with which a microtubule may have contact, most remain attached only briefly. This is illustrated in Fig. 11, which shows the integrated probability distribution of total attachment times. A small number of these motors remain attached for extended periods of time, forming the long tails of these distributions, and it seems reasonable to believe that these perform most of the work involved in moving the microtubule. What is clear from this figure is that, at higher density, more motors remain attached for longer periods of time: the tail is much longer at $\sigma_{\text{kin}} = 10\ \mu m^{-2}$ than at $\sigma_{\text{kin}} = 5\ \mu m^{-2}$.

Sticky motors

It has been found in experiments (J. Howard, University of Washington, private communication), that not all motors are identical: there is a natural variation in speed among motors of a given type and, in addition, some motors may, for some reason, not be fully functional. We have examined the effects of such nonuniformity in motor speed, in two different ways.

First, we allowed a motor to be either fast ($v_{\text{fast}} = 800$ nm s^{-1}) or slow ($v_{\text{slow}} = 200$ nm s^{-1}). We call this the delta-function velocity distribution. The fraction of slow motors, q, lies between 0 and 1. For $q = 0$, all the motors are fast, and for $q = 1$, they are all slow. Using the methods described previously, we measured the speed of the microtubule for several different values of kinesin densities, σ_{kin}, as q was increased from 0 to 1. The results are shown in Fig. 12 *A*. From Fig. 12 *A*, two things are clear: the overall behavior of the microtubule speed, as a function of q, is nonlinear; and a small admixture (say, $q \leq 0.1$) of slow motors has little effect on the overall speed of the microtubule. Likewise, a small admixture of fast motors ($q \geq 0.9$) has little effect.

We also looked at a more realistic scenario, in which the motor speeds are distributed according to a normal or Gaussian distribution. This is characterized by specifying a mean speed (v_{mean}) and a standard deviation from the mean (σ_{vel}). For the Gaussian distribution in motor speeds shown in Fig. 12 *B*, the principal effect of allowing the motors to

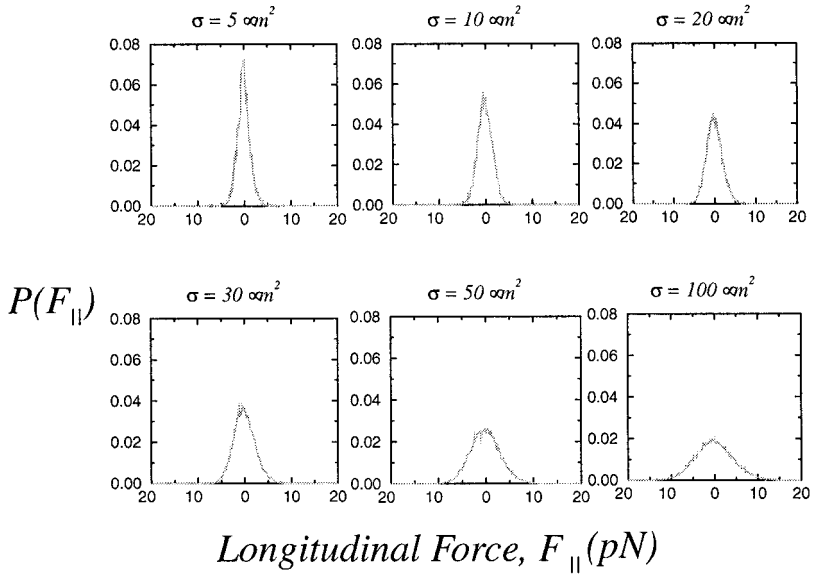

FIGURE 9 Distribution over time of the total force exerted on a MT. The labels in the panels in the figure indicate the kinesin densities of σ_{kin} = 5, 10, 20, 30, 50, and 100 μm^{-2}, respectively. It illustrates that the mean force exerted is always a very small fraction of the stall force, though the maximum instantaneous force exerted increases with kinesin density, and may be several times F_{stall}.

assume speeds over a wide distribution seems to be a slight increase in the mean speed for very wide distributions of motor speeds. It seems that, in general, the speed of the microtubule goes as the mean speed of the motors.

Theoretical analysis

One of the main results of this paper is the agreement between experiment and our numerical results, shown in Fig. 5. To provide further understanding to the agreement of these results, we have carried out approximate analytical calculations of the model Langevin Eqs. 6. We have analyzed the short and long time limits of the equations for one, two, and a very large number of motors attached to the MT. The details of these calculations are given in the Appendix. The analytic calculations differ from the numerical ones in that we do not consider the dynamic attachment and detachment of motors from the MT, but assume that the motors are attached all the time. We do find, nonetheless, that the asymptotic value of the average displacement velocity of the MT is given by the mean speed of the motors, that quantitatively agrees with the experiments and our numerical calculations.

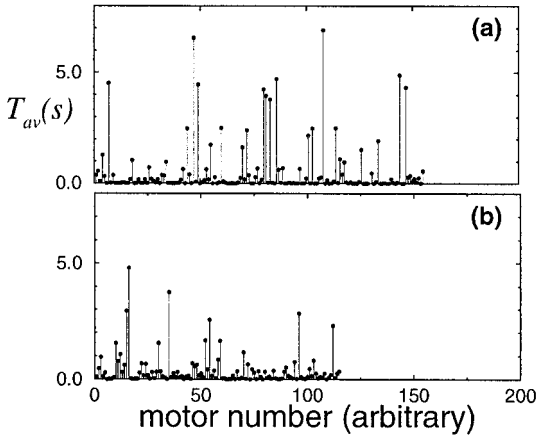

FIGURE 10 Histogram showing the length of time for which each motor is attached to the microtubule. The horizontal axis gives a unique number to every motor that has ever attached to the microtubule. The vertical axis indicates the total length of time for which this motor is attached during the course of the simulation (it may detach and then re-attach). (*a*) the results for σ_{kin} = 10 μm^{-2}; (*b*) those for σ_{kin} = 5 μm^{-2}. It is clear that only a small fraction of the motors remain attached for a significant length of time, indicating that a small number of them do most of the work. The total length of time for the run was 10 s.

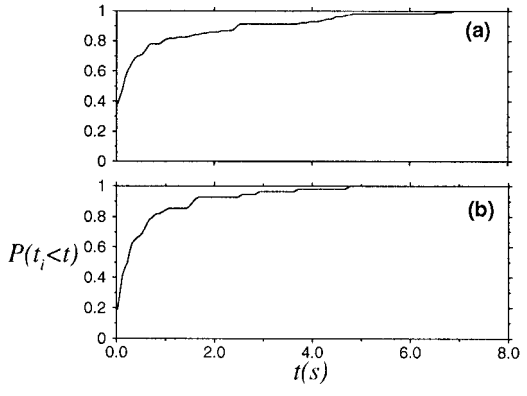

FIGURE 11 Integrated probability of attachment lifetimes. The abscissa $P(t_i < t)$ indicates the probability that any motor i will have a total attachment time less than the ordinate, t. The total length of time for the run was 10 s. (*a*) σ_{kin} = 10 μm^{-2}; (*b*) σ_{kin} = 5 μm^{-2}.

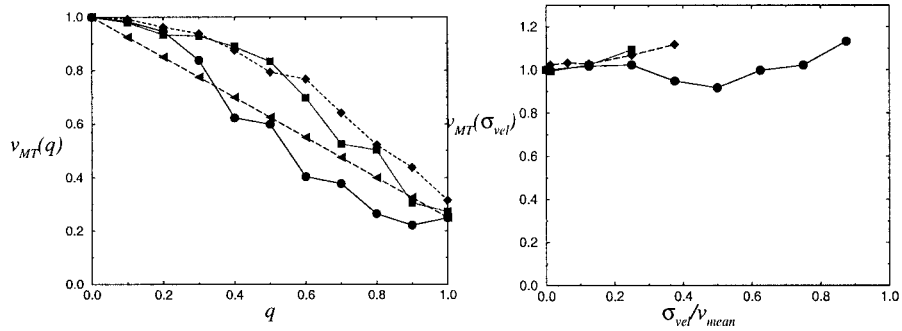

FIGURE 12 Effects of distribution in motor speeds on the MT velocity, at various kinesin densities. To compensate for the slight dependence of the MT velocity on kinesin density, all velocities at a given density have been normalized to the velocity for that density, with no distribution in speed. (*A*) Delta-function distribution $p(v) = (1 - q)\delta(v - v_{\text{fast}}) + q\delta(v - v_{\text{slow}})$. $v_{\text{fast}} = 800$ nm s^{-1}, and $v_{\text{slow}} = 200$ nm s^{-1}. Data for three different kinesin densities are shown: ●, ■, and ♦ represent data for $\sigma_{\text{kin}} = 10$, 40, and 100 μm s^{-1}, respectively. In addition, ◀ indicate the linear relationship $v = 1 - 0.75q$, which would be achieved if the MT speed varied linearly with q. (*B*) Gaussian distribution $p(v) = (2\pi\sigma_{\text{vel}}^2)^{-1/2} \exp(-(v - v_0)^2/2\pi\sigma_{\text{vel}}^2)$. Mean motor speed, v_0, is 800 nm s^{-1}, and the distribution width σ_{vel} is normalized to this value. Data for three different kinesin densities are shown: ●, ■, and ♦ represent data for $\sigma_{\text{kin}} = 10$, 60, and 100 μm^{-2}, respectively.

DISCUSSION

We have introduced a simplified stochastic model to describe the behavior of kinesin-based microtubule gliding assays. We set up a phenomenology-based theoretical description for the motion of a single microtubule moving through a viscous medium (assumed to be water), across a bed of attached kinesins. Comparing the results of our simulation and analytic analysis with those obtained experimentally (Howard et al., 1989; Hancock and Howard, 1998), we find rather good agreement. By analyzing the total force exerted by the motors on the microtubule as a function of time, we have shown how cancellations between the forces exerted by the individual motors can produce a resultant that is orders of magnitude smaller than the maximum force exerted by a single motor, but in agreement with the predicted value of the total force required to produce the experimentally observed motion. There are differences in the explicit expressions for the force used in numerical analysis, which yield results that compare with the experimental results, in contrast to the forces used in analytic calculations. These differences are, however, not important to explain the general qualitative property of having an almost constant MT displacement speed for different kinesin densities.

Our numerical analysis for the duration of each motor attachment to the microtubule reveals that, although a microtubule may come into contact with hundreds (at low kinesin densities) or thousands (at high kinesin densities) of motor molecules, only a small fraction of these remain attached for long periods of time, and therefore most of the work appears to be performed by a relatively small number of motors. We have also examined the effect of allowing a distribution in the maximum speeds of the motors, to mimic the natural nonuniformity in motor behavior. Taking a binomial distribution in motor speeds, where a fraction q of the motors have speed v_{slow} and the remaining motors have speed v_{fast}, we find that the microtubule speed generally scales with the average motor speed. Taking a Gaussian distribution, we find that the microtubule speed remains more or less unchanged. In each case, it seems that the speed of the microtubule is proportional to the mean maximum motor speed. Note that our mechanical model description does not contain biochemical elements that may also play a roll, like the energy consumption of ATP that depends on the total number of motors moving along the MT. We do find, however, a good semi-quantitative agreement between our model and experiment.

In summary, the goal of our work was first to come up with a simple mechanical model that can agree quantitatively with the experimental results (Howard et al., 1989; Svoboda et al., 1993; Hunt et al., 1994; Coppin et al., 1995) and with previous theoretical analysis (Duke et al., 1995). Second, we wanted to develop a model that we could use to study the more complicated mitotic spindle formation (J.-F. Chauwin, F. Gibbons, and J. José, manuscript in preparation). Previous theoretical analysis has also provided some understanding to this problem (Duke and Leibler, 1996). Here we show, however, that our simplified model can provide numerical results that are in good quantitative agreement with experiment. Furthermore, we also provided an approximate analytic understanding of the kinesin density independence of the MT averaged displacement velocity.

APPENDIX

Langevin equations for the microtubule dynamics

Following the standard treatment (Doi and Edwards, 1986) we decompose the translational hydrodynamical drag force in its parallel and perpendicular components. The parallel and perpendicular friction constants $\zeta_{\|}$ and $\zeta_{\perp}$ are not equal. Thus, if $\vec{v}_{\|}$ and $\vec{v}_{\perp}$ are the parallel and perpendicular components of the MT velocity $\vec{v}$, the drag is then written as

$$\vec{f} = \zeta_{\parallel}\vec{v}_{\parallel} + \zeta_{\perp}\vec{v}_{\perp}, \tag{A1}$$

where

$$\vec{v}_{\parallel} = (\vec{v}\cdot\hat{\vec{u}})\hat{\vec{u}}, \quad \vec{v}_{\perp} = \vec{v} - \vec{v}_{\parallel}, \tag{A2}$$

and $\vec{u} = \cos\Theta\hat{\imath} + \sin\Theta\hat{\jmath}$ being the unit vector pointing along the MT. Combining Eqs. A1 and A2, the components of the drag force can be written as

$$\begin{aligned} f_x &= v_x(\zeta_{\parallel}\cos^2\Theta + \zeta_{\perp}\sin^2\Theta) + v_y(\zeta_{\parallel} - \zeta_{\perp})\sin\Theta\cos\Theta, \\ f_y &= v_y(\zeta_{\parallel}\sin^2\Theta + \zeta_{\perp}\cos^2\Theta) + v_x(\zeta_{\parallel} - \zeta_{\perp})\sin\Theta\cos\Theta. \end{aligned} \tag{A3}$$

Inserting Eq. A3 in Eq. 1 and decomposing $\vec{F}$ and $\vec{\eta}(t)$ in their parallel and perpendicular components, as in Eq. A2, we obtain the following Langevin equations for the MT motion:

$$\begin{aligned} \dot{x} &= \frac{1}{\zeta_{\parallel}}[F_{\parallel} + \eta_{\parallel}(t)]\cos\Theta - \frac{1}{\zeta_{\perp}}[F_{\perp} + \eta_{\perp}(t)]\sin\Theta, \\ \dot{y} &= \frac{1}{\zeta_{\parallel}}[F_{\parallel} + \eta_{\parallel}(t)]\sin\Theta + \frac{1}{\zeta_{\perp}}[F_{\perp} + \eta_{\perp}(t)]\cos\Theta, \\ \dot{\Theta} &= \frac{1}{\zeta_r}[\tau + \eta_r(t)]. \end{aligned} \tag{A4}$$

To satisfy the fluctuation-dissipation theorem, the Langevin forces must obey the following Gaussian white noise correlation relations (Risken, 1996)

$$\langle\eta_i(t)\rangle = 0, \quad \langle\eta_i(t)\eta_j(t')\rangle = 2\delta_{ij}\zeta_i k_{\mathrm{B}}T\delta(t - t'), \tag{A5}$$

where the i, j indicate $\parallel$, $\perp$, or r. The symbol $\langle\cdots\rangle$ represents the time average, T the temperature, and k_{B} the Boltzmann constant. The diffusion coefficients for translation parallel and perpendicular to the rod and the diffusion coefficient for the angular motion are denoted by $D_{\parallel}$, $D_{\perp}$, and D_{r}, respectively, which must satisfy the Einstein relations

$$D_i = \frac{k_{\mathrm{B}}T}{\zeta_i}, \tag{A6}$$

Expressions for the friction coefficients $\zeta_{\parallel}$, $\zeta_{\perp}$ and ζ_r for a rod of length L and diameter $2b$ are given by (Doi and Edwards, 1986)

$$\begin{aligned} \zeta_{\parallel} &= \frac{2\pi\eta_W L}{\ln(L/b)}, \\ \zeta_{\perp} &= \frac{\zeta_{\parallel}}{2}, \\ \zeta_{\mathrm{r}} &= \frac{\pi\eta_W L^3}{3[\ln(L/b) - \gamma]}, \end{aligned} \tag{A7}$$

where $\gamma = 0.8$ is a constant and $\eta_W = 10^{-3}$ kg m^{-1} s^{-1} is the viscosity of water. We generally take the rod to be one-dimensional (i.e., having length, but no width). In computing the involved coefficients, however, we use the values shown in Table 1. From Eqs. A7, we get $\zeta_{\parallel} = 10^{-5}$ g s^{-1} and $\zeta_r = 2 \times 10^2$ g nm^2 s^{-1}.

Motor phenomenology

It has been shown experimentally (Svoboda et al., 1993) that kinesin can be modeled as a nonlinear (non-Hookean) spring, whose stiffness increases with extension. The optical trap they used in their experiment is found to obey Hooke's law, with spring constant (related to the laser power) of $k_{\mathrm{laser}} = (4.3 \pm 0.3) \times 10^{-4}$ pN nm^{-1} mW^{-1}. For the low-load part of their experiment (laser power $\sim$ 17 mW), this gives an effective spring constant for the trap of $k_{\mathrm{laser}}^{\mathrm{low\text{-}load}} \sim 7.31 \times 10^{-3}$ pN nm^{-1}. During the high-load part of their experiment, the power is increased to 58 mW, causing the spring constant to increase proportionately to $k_{\mathrm{laser}}^{\mathrm{high\text{-}load}} \sim 25 \times 10^{-3}$ pN nm^{-1}. By comparison, the spring constant associated with the kinesin itself varies from $k_s \sim 22 \times 10^{-3}$ pN nm^{-1} for a distance of 50 nm from the trap-center, to 53×10^{-3} pN nm^{-1} at the edge of the trap (200 nm from the center). In each case, the motor spring constant is larger than that associated with the optical trap (though not by a large factor). It has been found (Duke and Leibler, 1996), in simulations, that the force–extension relationship of the spring is nonlinear, with the force diverging for large extensions. They made use of the Langevin function $L(x) \equiv \coth x - 1/x$, but mention that any other sufficiently divergent function will also work. It seems that what they imply is that, beyond a certain extension, the force should diverge, effectively pulling the motor off the microtubule. Because the measured spring constant for kinesin varies only by a factor 2 from low- to high-load conditions, a linear approximation seems nonetheless quite reasonable. The nonlinearity (Duke and Leibler, 1996) is important only insofar as it causes the motor to detach from the MT once the load (or equivalently in our model, the extension) becomes too great. We account for this by detaching any motor that attempts to stretch beyond twice its own length. Many experimental workers have shown that kinesin obeys a force–velocity curve like the one shown in Fig. 8, in which the motor attains maximum speed when it is unloaded, with the speed dropping linearly as the load increases, up to a point. Beyond a certain load, called the *stall force*, forward motion becomes impossible. In experiments, no retrograde motion has been observed, although some models have predicted such behavior (Leibler and Huse, 1993).

Numerical simulations

It therefore seems reasonable to assume that the motor is pulled off the microtubule when the force exceeds the stall force, F_{stall}. In this numerical analysis, we used the linear relationship

$$v(F) = v_0\left(1 - \frac{F}{F_{\mathrm{stall}}}\right), \tag{A8}$$

subject to the condition that the velocity may not be negative. The specific values of v_0 and F_{stall} are given in Table 1. Experimental work (Hunt and Howard, 1993) has illuminated the nature of the coupling among the head, body, and tail of kinesin. In particular, they have shown that there must be a swiveling coupling between the head and body regions of this motor, because attachment between motor and microtubule is not dependent on relative orientation. In addition, there is evidence that the body region acts like a torsional spring, a "coiled coil," with stiffness $K = (117 \pm 19) \times 10^{-24}$ N m rad^{-1}. This is extremely weak, and it is unlikely that, once coiled, kinesin could completely uncoil itself during the detachment phase of its power cycle. Further evidence for the torsional spring model is given by the angular distribution of the microtubules—it is Gaussian rather than uniform, suggesting a smooth, symmetric potential well, rather than simply a pair of stops. Nearly 100% of the motors on the surface of an organelle that can reach the microtubule should be able to bind and exert force. With any motor, there is a finite probability that it will spontaneously detach from the microtubule. In contrast to other motors, however, kinesin has the property of *processivity*. This means that its duty ratio (the percentage of time the motor remains bound to the filament) is extremely high: >99%. This compares to a typical value of 5–20% for myosin (Finer et al., 1994).

We assume 100% processivity in this work. Perhaps the only nonintuitive parameter here is the *capture parameter, w*, shown in Table 1. It describes the Brownian rotational motion of the motors. Because they are so much smaller than the MTs, they diffuse on a much faster time scale. To see this, we just need to compute the rotational diffusion coefficient, taking the motors as rigid rods of length 80 nm and diameter 20 nm (Eqs. A7 and A6). We find that it comes out to $\sim 9600\ s^{-1}$. The time required to rotate through an angle π is $t \sim \pi^2/D_r \equiv 10^{-3}$ s (see Honerkamp, 1994, for an explanation of mean first-passage times). Thus, for time-steps of this order or larger, the rotational motion of the motors is completely blurred out. For this reason, we can assume that, once the MT is within a distance of about half the motor's length (i.e., 40 nm), the motor will rotate to a position that causes it to be close enough to the MT that it can attach. Our numerical simulations are based on Eq. 6 which can be obtained from Eqs. A4 combined with Eqs. 4 and 5.

The simulations were performed on our group's cluster of Alpha workstations (Digital Equipment Corp., Maynard, MA). With clock speeds ranging from 100 to 433 MHz, these RISC machines are capable of ~18–140 MFLOPS (million floating-point operations per second). The programming languages used were Fortran 90 (numerical work) and C (input/output), compiled using Digital Equipment Corporation's compilers (f90 V4.1-270 and cc V5.2-036, respectively). In addition, the Unix Per1 language (version 5.003) was used for data processing. The choice of programming language was motivated by the desire to take advantage of such concepts as user-defined data types, which greatly ease the task of modeling such complex objects as molecular motors, without sacrificing the proven numerical efficiency of the Fortran language. In simulating noisy systems, we must be careful about the finite-difference method we use, and, in particular, about how it may influence the noise autocorrelations. This problem has been examined in detail (Helfand, 1979; Greenside and Helfand, 1981). We have used their second-order Runge–Kutta method to solve all the equations.

In this, as in all simulations, the question arises: What is the appropriate time-scale, τ? There are several considerations here: At very low density, the time-step should be short enough that the distance diffused by the rod in one step is not greater than the spring length, because this will cause unnatural (unrealistic) detachments of the springs from the rod. This imposes the limit $\tau \ll L_0^2/D$, where L_0 is the spring equilibrium length, and D is the diffusion coefficient of the MT. For the values considered here, this means that $\tau < 0.025$ s. In contrast, at very high density, if there is a large number of motors attached to the rod, we should take care that the time step is small enough that the combined force of all the motors does not cause overly jerky motion of the MT (it is a stochastic system), inducing spurious detachments. This means that we wish to have $\tau\dot{x} \equiv \tau\langle F\rangle D/k_BT \ll L_0$, where $\dot{x}$ is the instantaneous velocity of the MT center of mass, and $\langle F\rangle$ indicates the mean force felt by the MT as a result of all the motors. We write this as $\langle F\rangle \sim N_{att}\bar{f}$, where $\bar{f}$ is a time-averaged force for one motor. As an order-of-magnitude estimate, we might set this at $0.2F_{stall}$. For high kinesin density, $N_{att} = L\sigma_{kin}w$, where w is the capture parameter, and σ_{kin} is the kinesin density. This leads us to the upper limit on h,

$$\tau < L_0 \frac{k_BT}{D}\frac{1}{N_{att}\bar{f}} \equiv L_0 \frac{k_BT}{D}\frac{1}{L\sigma_{kin}w\bar{f}}.$$

For typical values used in this work (see Table 1), $\tau \sim 80/\sigma_{kin}w$. Clearly, the time-step (h) is to be chosen much smaller than this value. In simulating this system for high kinesin densities, the number of motors rapidly becomes very large, yet only a tiny fraction are attached to the MT at a given instant. In addition, because the motion is noisy only on a small scale at biological temperatures, the particular set of motors that are attached does not vary a lot from one instant to another. Maintaining a linked-list (see Brainerd et al., 1996, for details of implementation in Fortran 90) of attached motors greatly speeds things up. At each time step, we iterate over all the motors, to see if they can attach to the MT. If so, we add them to the list of attached motors. If not, we do nothing. After all the motors have been checked, we compute the forces exerted by the attached motors. The savings in computing forces for such a small fraction of motors greatly outweighs the cost of maintaining the list.

Theoretical analysis

Here we obtain approximate analytical results from Eqs. A4. It is convenient first to perform a coordinates transformation of the center of mass. Making a rotation of the $\hat{x}$ and $\hat{y}$ axis by an angle Θ, we obtain the coordinates,

$$q = x\cos\Theta + y\sin\Theta,$$
$$p = -x\sin\Theta + y\cos\Theta, \tag{A9}$$

which give the parallel (q) and perpendicular (p) components of the center of mass $\vec{R}$. Transforming Eq. A4 using these new variables, we get the nonlinear Langevin equations,

$$\dot{q} - \frac{F_\parallel}{\zeta_\parallel} - p\frac{\tau}{\zeta_r} = \frac{\eta_\parallel(t)}{\zeta_\parallel} + p\frac{\eta_r(t)}{\zeta_r},$$
$$\dot{p} - \frac{F_\perp}{\zeta_\perp} + q\frac{\tau}{\zeta_r} = \frac{\eta_\perp(t)}{\zeta_\perp} - q\frac{\eta_r(t)}{\zeta_r},$$
$$\dot{\Theta} - \frac{1}{\zeta_r}\tau = \frac{1}{\zeta_r}\eta_r(t), \tag{A10}$$

which will be the basis for our subsequent analysis. From Fig. 1, one sees that $\vec{h}_i = \vec{R} + \vec{\alpha}$, where $\vec{\alpha}$ is a vector pointing along the plus end of the MT. To model the uniform walking of the ith motor, we assume that

$$\alpha^{(i)} = \alpha_0^{(i)} + v_m^{(i)}t, \tag{A11}$$

where $v_m^{(i)}$ is the mean speed of the ith motor walking along the MT, and $\alpha_0^{(i)}$ is its initial attachment position. Here all the velocities $v_m^{(i)}$ are chosen positive because the kinesins are plus-end-directed motors. Note that the model is independent of an underlying mechanism for the walking because it does not include any kind of stepwise movement. The only assumption is that the kinesin remains bound to the MT throughout the motion, like the wild-type kinesins (Hancock and Howard, 1998). This assumption allows us to fix the mean speed $v_m^{(i)}$ for each motor. Note that the inclusion of this (linear) term allows us to mimic the velocity of the motors as they consume ATP. Using Eqs. 4 and 5, the parallel and perpendicular force components and the torque can be expressed in terms of the (q, p, Θ) coordinates system as

$$F_\parallel^{(i)} = -k_s(q + \alpha^{(i)}(t) - r_\parallel^{(i)}),$$
$$F_\perp^{(i)} = -k_s(p - r_\perp^{(i)}),$$
$$\tau^{(i)} = -k_s\alpha^{(i)}(t)(p - r_\perp^{(i)}), \tag{A12}$$

where

$$r_\parallel^{(i)} = r_x^{(i)}\cos\Theta + r_y^{(i)}\sin\Theta,$$
$$r_\perp^{(i)} = -r_x^{(i)}\sin\Theta + r_y^{(i)}\cos\Theta. \tag{A13}$$

Here we try to understand the relation between the MT speed and the attached motors speed. We start by analyzing the MT motion due to only one attached motor. In this case, after setting $\vec{r} = 0$ and $\alpha(t) = \alpha_0 + v_m t$, the Langevin equations for the MT become

$$\dot{q} + \kappa(q + \alpha(t)(1 + \varepsilon p^2)) = D_\parallel^{1/2}(\gamma_\parallel(t) + p\varepsilon^{1/2}\gamma_r(t)),$$

$$\dot{p} + \kappa p(2 - \varepsilon\alpha(t)q) = D_\parallel^{1/2}(2^{1/2}\gamma_\perp(t) - q\varepsilon^{1/2}\gamma_r(t)),$$

$$\dot{\Theta} + \kappa\alpha(t)\varepsilon p = D_r^{1/2}\gamma_r(t), \qquad \text{(A14)}$$

where we have set $\kappa \equiv k_s/\zeta_\parallel$ and $\varepsilon \equiv \zeta_\parallel/\zeta_r$. The white Gaussian noise sources are normalized as $\gamma_r(t) \equiv \eta_i(t)/(\zeta_i D_i^{1/2})$, to satisfy $\langle\gamma_i(t)\gamma_j(t')\rangle = 2\delta_{ij}\delta(t - t')$. Using the calculated coefficients $\zeta_\parallel$ and ζ_r, we find that $\kappa = 2 \times 10^3\ \mathrm{s}^{-1}$ and $\varepsilon = 5.3 \times 10^{-8}\ \mathrm{nm}^2$. With these coefficients in mind, and noting that, if the fixed tail of the motor is attached at $\vec{r} = 0$, the values of q and p cannot be larger than $2L_0$ (so that the motor remains attached to the MT). We can then neglect the terms proportional to ε in Eq. 20, so that

$$\dot{q} + \kappa(q + \alpha(t)) = D_\parallel^{1/2}\gamma_\parallel(t),$$

$$\dot{p} + 2\kappa p = (2D_\parallel)^{1/2}\gamma_\perp(t),$$

$$\dot{\Theta} + \kappa\alpha(t)\varepsilon p = D_r^{1/2}\gamma_r(t). \qquad \text{(A15)}$$

To obtain the average MT speed we need to calculate

$$\langle V_{\mathrm{MT}}\rangle = \frac{\mathrm{d}}{\mathrm{d}t}\langle\vec{R}^2\rangle^{1/2}. \qquad \text{(A16)}$$

We need then to find the evolution of $\langle q^2\rangle$ and $\langle p^2\rangle$, because the mean square displacement of the center of mass is given by $\langle\vec{R}^2\rangle = \langle x^2\rangle + \langle y^2\rangle = \langle q^2\rangle + \langle p^2\rangle$. After integration and averaging over time of Eqs. A15, we get

$$\langle q^2\rangle = \left[\alpha_0(1 - e^{-\kappa t}) - q_0 e^{-\kappa t} + \frac{v_m}{\kappa}(e^{-\kappa t} - 1 + \kappa t)\right]^2 + \frac{D_\parallel}{\kappa}(1 - e^{-2\kappa t}),$$

$$\langle p^2\rangle = p_0^2 e^{-4\kappa t} + \frac{D_\parallel}{\kappa}(1 - e^{-4\kappa t}), \qquad \text{(A17)}$$

where κ^{-1} is the characteristic decaying time associated with the Hookean behavior of the motors. This time is of the order of 1 ms. Therefore, for times greater than κ^{-1}, the mean square displacement of the center of mass tends to

$$\langle\vec{R}^2\rangle = \frac{2D_\parallel}{\kappa} + (\alpha_0 + v_m t)^2, \qquad \text{(A18)}$$

so that the average speed $\langle V_{\mathrm{MT}}\rangle$ tends to the mean motor speed v_m.

In contrast, for $\kappa t \gg 1$, the evolution equation for the averaged mean square of the angle Θ reads

$$\langle\Theta^2\rangle \to \Theta_0^2 - \varepsilon p_0\Theta_0\left(\alpha_0 + \frac{v_m}{2\kappa}\right) + \left(\frac{\varepsilon}{2}\right)^2\left[\left(p_0 - \frac{D_\parallel}{2\kappa}\right)\left(\alpha_0 + \frac{v_m}{2\kappa}\right)^2 + \frac{D_\parallel}{\kappa}\left(\alpha_0^2 + \left(\frac{v_m}{2\kappa}\right)^2\right)\right] + 2D_r t + \varepsilon^2\frac{D_\parallel}{2}\left[\left(\alpha_0 - \frac{v_m}{2\kappa}\right)\alpha_0 t + \left(\alpha_0 - \frac{v_m}{4\kappa}\right)v_m t^2 + \frac{1}{3}v_m^2 t^3\right]. \qquad \text{(A19)}$$

This result is strongly dependent on the initial attachment position α_0 along the MT, that affects the value of the rotational angular motion produced by the torque. Note that setting $\vec{F} = 0$ in Eqs. A10 (i.e., the motor is detached), we have

$$\langle\vec{R}^2\rangle = 2(D_\parallel + D_\perp)t, \quad \langle\Theta^2\rangle = 2D_r t, \qquad \text{(A20)}$$

and then $\langle V_{\mathrm{MT}}\rangle \sim 0$, because, in this case, the MT diffuse away in the solution performing a pure Brownian motion.

The case of two motors attached to the MT can be analytically solved by setting $r_x^1 = r_x^2 = 0$ and $r_y^1 = -r_y^2$. Following closely similar steps as above, we find

$$\langle\vec{R}^2\rangle \to \frac{D_\parallel}{\kappa} + \left[\left(\frac{v_1 + v_2}{4\kappa} - \frac{\alpha_1^0 + \alpha_2^0}{2}\right) - \frac{v_1 + v_2}{2}t\right]^2, \qquad \text{(A21)}$$

where we can see that the MT speed also tends to the average of the two motor velocities. When we consider N motors that are attached to the MT, the corresponding Langevin equations read

$$\dot{q} + \kappa N\left\{q + \sum_i{}' \frac{1}{N}(\alpha^{(i)}(t) - r_\parallel^{(i)}) + \varepsilon p\left(p\sum_i{}' \frac{1}{N}\alpha^{(i)}(t) - \sum_i{}' \frac{1}{N}\alpha^{(i)}(t)r_\perp^{(i)}\right)\right\} = D_\parallel^{1/2}(\gamma_\parallel(t) + \varepsilon^{1/2}p\gamma_r(t)),$$

$$\dot{p} + 2\kappa N\left\{p - \sum_i{}' \frac{1}{N}r_\perp^{(i)} - \varepsilon\frac{q}{2}\left(p\sum_i{}' \frac{1}{N}\alpha^{(i)}(t) - \sum_i{}' \frac{1}{N}\alpha^{(i)}(t)r_\perp^{(i)}\right)\right\} = D_\parallel^{1/2}(2^{1/2}\gamma_\perp(t) - \varepsilon^{1/2}q\gamma_r(t)),$$

$$\dot{\Theta} + \varepsilon\kappa\left\{p\sum_i{}' \alpha^{(i)}(t) - \sum_i{}' \alpha^{(i)}(t)r_\perp^{(i)}\right\} = D_r^{1/2}\gamma_r(t), \qquad \text{(A22)}$$

where Σ_i' denotes the sum only over those motors that are attached to the MT. Using the same approximations as in the case of only one attached motor, we get

$$\dot{q} + \kappa N\left\{q + \sum_i{}' \frac{1}{N}(\alpha^{(i)}(t) - r_\parallel^{(i)})\right\} = D_\parallel^{1/2}\gamma_\parallel(t),$$

$$\dot{p} + 2\kappa N\left\{p - \sum_i{}' \frac{1}{N}r_\perp^{(i)}\right\} = (2D_\parallel)^{1/2}\gamma_\perp(t), \qquad \text{(A23)}$$

which, after time integration and averaging, give

$$\langle q^2\rangle = q_0^2 e^{-2N\kappa t} + \frac{D_\parallel}{N\kappa}(1 - e^{-2N\kappa t}) - 2q_0 e^{-N\kappa t}\sum_i{}' \frac{1}{N}\left(\left(\alpha_0^{(i)} - \frac{v_m^{(i)}}{N_\kappa}\right)(1 - e^{-N\kappa t}) + v_m^{(i)}t\right) + \left[\sum_i{}' \frac{1}{N}\left(\left(\alpha_0^{(i)} - \frac{v_m^{(i)}}{N_\kappa}\right)(1 - e^{-N\kappa t}) + v_m^{(i)}t\right)\right]^2,$$

$$\langle p^2\rangle = p_0^2 e^{-4N\kappa t} + \frac{D_\parallel}{N\kappa}(1 - e^{-4N\kappa t}). \qquad \text{(A24)}$$

Here we used the fact that, in the high kinesin density case, it is reasonable to discard those terms that include $\Sigma_i'\langle r_\parallel^{(i)}\rangle$ and $\Sigma_i'\langle r_\perp^{(i)}\rangle$, because

we have assumed that the kinesins are randomly located in the plane. For the short time evolution, we find

$$\langle \vec{R}^2 \rangle = \langle \vec{R}_0^2 \rangle + [6D_\parallel - 2N\kappa(q_0^2 + 2p_0^2)]t, \quad \text{(A25)}$$

which shows that, initially, the motion is Brownian, in agreement with our numerical results. In contrast, note from Eqs. A24 that the characteristic relaxation time for the high kinesin density case is $(N\kappa)^{-1}$, which is very short and difficult to observe experimentally.

For $N\kappa t \gg 1$ the mean square displacement of the center of mass tends to

$$\langle \vec{R}^2 \rangle = \frac{2D_\parallel}{N\kappa} + \left[\sum_i{}' \frac{1}{N} (\alpha_0^{(i)} + v_m^{(i)} t) \right]^2, \quad \text{(A26)}$$

and, taking into account that, for high motors densities, one can set $\Sigma_i' \alpha_0^{(i)} \approx 0$, we finally get

$$\langle \vec{R}^2 \rangle = \frac{2D_\parallel}{N\kappa} + \left[\sum_i{}' \frac{v_m^{(i)}}{N} t \right]^2, \quad \text{(A27)}$$

from which we conclude that the MT speed tends to the average value $\Sigma_i' v_m^{(i)}/N$ of the attached motor speeds.

We note that, in the gliding-assay experiments (Howard et al., 1989; Hancock and Howard, 1998) and in our numerical simulations, the MT motion is essentially one-dimensional due to the compensation of the perpendicular motor forces acting on the MT. If one sets $\Theta = \Theta_0 = 0$, then $q = x$ and the MT motion can be described simply by

$$\dot{x} = -\kappa N \left[x + \sum_i{}' \frac{1}{N} (\alpha^{(i)}(t) - r_x^{(i)}) \right] + D_x^{1/2} \gamma_x(t), \quad \text{(A28)}$$

from which we obtain

$$\langle x^2 \rangle = \frac{D_\parallel}{N\kappa} (1 - e^{-2N\kappa t}) + \left[\sum_i{}' \frac{1}{N} \alpha_0^{(i)} (1 - e^{-N\kappa t}) - x_0 e^{-N\kappa t} + \sum_i{}' \frac{v_m^{(i)}}{N^2 \kappa} (e^{-N\kappa t} - 1 + N\kappa t) \right]^2, \quad \text{(A29)}$$

where we neglected those terms that include $\Sigma_i' \langle r_x^{(i)} \rangle$.

For $N\kappa t \gg 1$, expression A29 tends to

$$\langle x^2 \rangle = \frac{D_\parallel}{N\kappa} + \left[\sum_i{}' \frac{1}{N} (\alpha_0^{(i)} + v_m^{(i)} t) \right]^2, \quad \text{(A30)}$$

and we recover the experimental and numerical results for which the velocity of the MT is given by the average of the attached motor speeds. Note that this result is independent of the form of the velocity distribution. It is worth pointing out that, in our analytical analysis, we assumed that the N motors are always attached to the MT. As the MT moves, however, new motors are attached at its leading end and others are detached at the tail.

Finally, we analyze the behavior of the force exerted by the motor. From (Eq. A12), the mean value of the longitudinal force can be calculated from

$$\langle F_\parallel \rangle = -k_s \left(N\langle q \rangle + \sum_i{}' (\alpha^{(i)}(t) - \langle r_\parallel^{(i)} \rangle) \right), \quad \text{(A31)}$$

which includes the mean displacement $\langle q \rangle$. Time integration and averaging of Eq. A23 gives, for $N\kappa t \gg 1$,

$$\langle q \rangle = -\sum_i{}' \frac{1}{N} (\alpha_0^{(i)} + v_m^{(i)} t). \quad \text{(A32)}$$

Plugging in numbers to this equation, we get

$$\langle F_\parallel \rangle = -\zeta_\parallel \sum_i{}' \frac{v_m^{(i)}}{N} \approx -0.065\text{pN}, \quad \text{(A33)}$$

where we use that $\Sigma_i' v_m^{(i)}/N \approx 650$ nm s^{-1}, and quantitatively corresponds to the numerical result.

Our approximate analysis has helped our understanding of why the MT motion is almost kinesin density independent. From our analysis we see, however, that we have left out many collective effects that will be kinesin density dependent. We could conceive more complicated analysis of the equations of motion that could lead to further probes of the experimental results. We leave that for future study.

We thank Prof. William Dietrich, III and Angela Ramsey of the Biology Department at Northeastern University for helpful discussions. Suggestions by Jonathon Howard at the University of Washington were very useful toward completion of this work. Thanks are also due to Jagesh Shah and Paul Janmey of the Division of Experimental Medicine at Brigham and Women's Hospital for being generous with their time, and showing us their experimental setup. This work has been partially funded by the Center for Interdisciplinary Research on Complex Systems, Northeastern University fund.

REFERENCES

Alberts, B., D. Bray, J. Lewis, M. Raff, K. Roberts, and J. D. Watson. 1994. Molecular Biology of the Cell. 3rd ed., Garland Publishing, Inc., New York.

Berg, H. C. 1983. Random Walks in Biology. 2nd ed., Princeton University Press, Princeton, NJ.

Block, S. M., L. S. B. Goldstein, and B. J. Schnapp. 1990. Bead movement by single kinesin molecules studied with optical tweezers. *Nature.* 348:348–352.

Brainerd, W. S., C. H. Goldberg, and J. C. Adams. 1996. Programmer's Guide to Fortran 90. Springer, New York.

Coppin, C. M., J. T. Finer, J. A. Spudich, and R. D. Vale. 1995. Measurement of the isometric force exerted by a single kinesin molecule. *Biophys. J.* 68:242s–244s.

Coy, D., M. Wagenbach, and J. Howard. 1999. Kinesin takes one 8-nm step for each ATP that it hydrolyses. *J. Biol. Chem.* 274:3667–3671.

Derényi, I., and T. Vicsek. 1996. The kinesin walk: a dynamic model with elastically coupled heads. *Proc. Natl. Acad. Sci. U.S.A.* 93:6775–6779.

Doi, M., and S. F. Edwards. 1986. The Theory of Polymer Dynamics. Clarendon Press, Oxford.

Duke, T., T. E. Holy, and S. Leibler. 1995. "Gliding assays" for motor proteins: a theoretical analysis. *Phys. Rev. Lett.* 74:330–333.

Duke, T., and S. Leibler. 1996. Motor protein mechanics: a stochastic model with minimal mechanochemical coupling. *Biophys. J.* 71: 1235–1247.

Finer, J. T., R. M. Simmons, and J. A. Spudich. 1994. Single myosin molecule mechanics: piconewton forces and nanometre steps. *Nature.* 368:113–119.

Gliksman, N. R., R. V. Skibbens, and E. D. Salmon. 1993. How the transition frequencies of microtubule dynamic instability (nucleation, catastrophe, and rescue) regulate microtubule dynamics in interphase and mitosis: analysis using a Monte Carlo computer simulation. *Mol. Biol. Cell.* 4:1035.

Greenside, H. S., and E. Helfand. 1981. Numerical integration of stochastic differential equations: II. *Bell Syst. Tech. J.* 60:1927–1940.

Hancock, W., and J. Howard. 1998. Processivity of the motor protein requires two heads. *J. Cell Biol.* 140:1395–1405.

Helfand, E. 1979. Numerical integration of stochastic differential equations. *Bell Syst. Tech. J.* 58:2289–2299.

Hirokawa, N. 1998. Kinesin and dynein superfamily proteins and the mechanism of organelle transport. *Science.* 279:519–526.

Hirokawa, N., K. K. Pfister, H. Yorifuji, M. C. Wagner, S. T. Brady, and G. S. Bloom. 1989. Submolecular domains of bovine brain kinesin identified by electron microscopy and monoclonal antibody decoration. *Cell.* 56:867–878.

Honerkamp, J. 1994. Stochastic Dynamical Systems. VCH Publishers, New York.

Howard, J., A. J. Hudspeth, and R. D. Vale. 1989. Movement of microtubules by single kinesin molecules. *Nature.* 342:154–158.

Hua, W., E. C. Young, M. L. Fleming, and J. Gelles. 1997. Coupling of kinesin steps to ATP hydrolysis. *Nature.* 388:390–393.

Hunt, A. J., F. Gittes, and J. Howard. 1994. The force exerted by a single kinesin molecule against a viscous load. *Biophys. J.* 67:766–781.

Hunt, A. J., and J. Howard. 1993. Kinesin swivels to permit microtubule movement in any direction. *Proc. Natl. Acad. Sci. U.S.A.* 90: 11653–11657.

Leibler, S., and D. A. Huse. 1993. Porters versus rowers: a unified stochastic model of motor proteins. *J. Cell Biol.* 121:1357–1368.

Lodish, H., D. Baltimore, A. Berk, S. L. Zipursky, P. Matsudaira, and J. Darnell. 1995. Molecular Cell Biology. 3rd ed., Scientific American Books, New York.

Peskin, C. S., and G. F. Oster. 1995. Force production by depolymerizing microtubules: load–velocity curves and run–pause statistics. *Biophys. J.* 69:2268.

Purcell, E. M. 1977. Life at low Reynolds number. *Am. J. Phys.* 45:3–11.

Risken, H. 1996. The Fokker-Planck equation. Springer, New York.

Schnitzer, M. J., and S. M. Block. 1997. Kinesin hydrolyses one ATP per 8-nm step. *Nature.* 388:386–390.

Scholey, J. M., J. Heuser, J. T. Yang, and L. S. B. Goldstein. 1989. Identification of globular mechanochemical heads of kinesin. *Nature.* 338:355–357.

Svoboda, K., C. F. Schmidt, B. J. Schnapp, and S. M. Block. 1993. Direct observation of kinesins stepping by optical trapping interferometry. *Nature.* 365:721–727.

Vicsek, T. 1997. A statistical physicist's approach to biological: from the kinesin walk to muscle. *In* Bulletin of the American Physical Society March meeting, Kansas City, MO. American Physical Society, College Park, MD.